A model-based oscillation suppression approach for a cable-suspended dual-arm aerial manipulator

Giancarlo D'Ago[1,3], Mario Selvaggio[1], Chiara Marzio[1], Luca Rosario Buonocore[3], Alejandro Suarez[2], Antonio Gonzalez-Morgado[2], Jose Villanueva[2], Anibal Ollero[2], Fabio Ruggiero[1]

***Abstract*— In aerial manipulators, the presence of cables between the aerial platform and the articulated system is beneficial to increase the distance between rotors' blades and the obstacles in the workspace and absorb unavoidable impacts arising during the interaction with the environment. However, cables also produce pendulum-like oscillatory behaviour due to dynamic coupling and to the effect of external forces when the robot navigates in free space through the environment. This paper presents a model-based control approach for the suppression of oscillations in cable-suspended dual-arm aerial manipulators. Contrary to many oscillation suppression techniques that act on the suspension platform, we exploit the dynamics of the articulated system to achieve the same goal. A linear controller is devised applying a partial feedback linearization technique for the unactuated variables of our system, i.e. the cables. Simulation and experimental tests are carried out using a quadrotor equipped with a cable-suspended dual-arm system to validate our proposed framework. With our control technique, drone-induced oscillations were reduced by up to 89%, with a settling time of 2.5 seconds.**

I. Introduction

In recent decades, the advent of Unmanned Aerial Vehicles (UAVs) has brought a transformative impact on various industries, as this type of technology makes it possible to perform inspection tasks that were previously impractical or dangerous. As a natural progression, robotic manipulators have been integrated into UAVs, giving rise to the Unmanned Aerial Manipulators (UAM) field [1]. This evolution enables these vehicles not only to perform visual inspections but also to engage in manipulation activities at significant altitudes and over long distances. The employment of a robotic arm allows dexterity and capability of manipulating objects. Consequently, these systems find application in the inspection and maintenance of challenging-to-access sites and structures, such as bridges, power lines, and pipe arrays in chemical plants. The use of manipulators in these scenarios can substitute manual intervention, thereby mitigating human risks [2], [3].

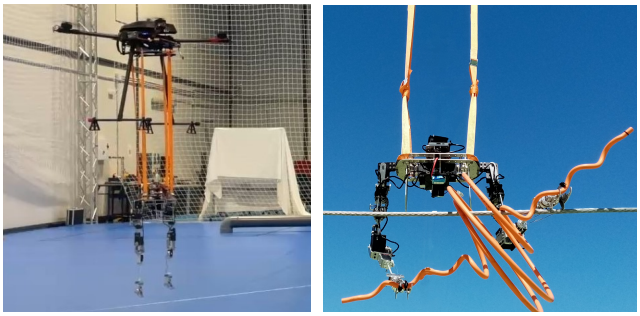

(a) (b)

Fig. 1. (a) The cable suspended dual-arm UAM system considered in this work. (b) Example of task (installation of bird diverters on a high-voltage line) carried out by the robot.

A new frontier in UAMs is the development of cable-suspended long-reach manipulators, i.e. robots typically consisting of an aerial suspension platform carrying an articulated system, usually dual-arm, in a pendulum configuration via cable suspension [4]–[6], as shown in Fig. 1(a). This configuration separates the aerial transportation platform from the handling system and has the great advantage of drastically extending the robot's workspace by means of a non-rigid connection with a relatively small added weight. This, above all, guarantees greater resilience towards impacts and collisions, particularly for tasks involving interaction with the environment [6]–[8]. Despite its many advantages, the presence of passive cables with small mass and low stiffness introduces uncontrolled second-order dynamics and imposes intricate unilateral constraints between the aerial platform and the articulated system. These oscillations may arise from several factors, including wind perturbations, contact forces, manipulator-induced wrenches, or aerial platform accelerations. In particular, during the transport of the system to the operation point, the motion of the aerial platform causes unavoidable sway of the suspended load, limiting the immediate use of the robot once it arrives at its destination. Is then necessary to wait for the system to stabilise completely before performing the manipulation task (such as the one shown in Fig. 1(b), thus increasing the total operation time. From a physical point of view, this is related to the fact that the connected systems have a non-negligible dynamic coupling, which causes a displacement of the load from its rest position. However, just like the movement of the drone, the movement of the articulated system also impacts the

The research leading to these results has been supported by the European Union's Horizon 2020 research and innovation program under the Marie Skłodowska-Curie (AERO-TRAIN, grant agreement No 953454), the European ROBotics and AI Network (euROBIN, grant agreement No 101070596), and the AI-DROW project, in the frame of the PRIN 2022 research program, grant n. 2022BYSBYX, funded by the European Union Next-Generation EU. The authors are solely responsible for its content.

[1] The authors are with the PRISMA Lab, Department of Electrical Engineering and Information Technology, University of Naples Federico II, Via Claudio 21, Naples, 80125, Italy. Corresponding author's email: giancarlo.dago@unina.it.

[2] The authors are with the GRVC Robotics Labs at the University of Seville, Camino de los Descubrimientos, Seville, 41092, Spain.

[3] The authors are with the European Organization for Nuclear Research, CERN, Espl. des Particules 1, Meyrin, 1211, Switzerland.

overall dynamics of the system.

With this motivation, in this article, we propose a model-based control technique for the suppression of oscillations through the action of the articulated system of a cable-suspended long-reach manipulator. The system under study is an aerial cable-suspended dual-arm system used to install bird diverters on high-voltage power lines [9], [10] (see Fig. 1(b)). In this system, four belts, tied in a parallel pattern to a drone and a lower platform, hold the shoulder structure of a lightweight and compliant anthropomorphic dual arm system (LiCAS A1 [11]). For such system, we devised a control technique to partially linearise and control the portion of the dynamics corresponding to the passive degrees of freedom (DoFs) of our system, i.e. the cables. Reduced models are used to preserve the strong inertial coupling property of the system. Contrary to many works that use the upper suspension platform trajectories to generate oscillation-free movements, we employ the movements of the arms to achieve the same scope. This is indeed useful when it is not convenient or possible to modify the controller of the upper platform. Moreover, arms control is more accurate and provides faster dynamics than the multi-rotor, which has higher inertia. Therefore, the arms allow to achieve more fine control of the oscillation, although with lower energy capacity compared to the multi-rotor. Simulation and experimental tests are carried out for the considered system to validate our proposed framework. The obtained results can be further appreciated in the video accompanying this article.

II. Related works

As stated in Section I, aerial systems relying solely on articulated manipulators rigidly attached to the drone may prove inadequate in maintaining a safe distance between the rotors and the areas being inspected [12]–[14]. Long-reach [5], [7], [8] and cable-suspended [6], [15], [16] aerial manipulators provide extended reach to expand the robot workspace and concurrently mitigate other effects arising from the interaction of the manipulator with the environment, for example insulating electrically the aerial platform during the realisation of maintenance tasks on live power lines [8], [9]. The integration of spring elements in the manipulator's joints and/or the utilisation of flexible suspension cables is a potential solution to mitigate these issues, as suggested by prior research [7], [17], [18]. Nevertheless, the presence of cables causes an oscillatory behaviour during the transport that needs to be avoided or reduced. One possibility to mitigate the swaying problem is to act directly on the suspension platform and intelligently control its movement.

Control of the load's swaying is a problem that has been widely studied in logistics, and in particular for crane transportation. These controls involve the direct modification of the trajectory driven by the crane by following different approaches. In [19] and [20] a comprehensive overview of anti-sway techniques for industrial overhead cranes is presented. Control methods can be divided into two broad categories: closed-loop control and open-loop control. Closed-loop approaches include PID control [21], fuzzy control [22], sliding mode [23], model-predictive control [24] and non-linear control [25]. Open-loop controls, on the other hand, include approaches based on input shaping [26], trajectory planning [27] and strategies based on neural networks [28]. Similar considerations can be made when the overhead crane is replaced by an aerial suspension platform, i.e. a drone, as in the case under study. In a parallel manner, although fewer works have been published on the topic so far, anti-sway approaches involving drone control can be closed-loop, such as the model-predictive control in [29], time-delayed proportional control of [30] or Lyapunov-based PID controller in [31], or open-loop approaches as in [32], [33].

However, all of the above-mentioned work relies on the operation of the suspension platform, and thus on a necessary modification of their controller, which cannot always be performed. Replacing the drone also involves reprogramming the control and, depending on the approach, rework of the model. To overcome these limitations, the presence of an actuated suspended load provides a viable solution. The idea is in fact to use the manipulator itself, whose controller can give access to the lowest level of commands (i.e. torque control), to suppress the oscillations generated by the transport. The adoption of actuated masses for sway control has been explored for example in [34] and [35] where a moving mass has been installed on the spreader of the suspension mechanism of a container, and its movement imparts an inertial force to the spreader that results in a suppression of undesired sway during crane transport. In [36] the addition of a controlled inertial disc system allows the suppression of oscillations of a flexible beam mounted vertically on an omnidirectional robotic platform. However, these works involve hardware modifications, which are often tedious and require system mechanical design and modelling process. In the presence of actuated loads, however, the addition of external masses is unnecessary, since the manipulators themselves can be used to suppress oscillations. A previous work dealing with oscillation suppression through the actuation of robotic manipulators can be found in [37] in which one of two manipulators mounted on the opposite faces of a fixed cable-suspended platform is used for oscillation compensation through a passivity-based approach. In this work, however, the transport platform is absent, and the robot on the upper face cannot be lately exploited for handling tasks. In [38], instead, a model-free approach based on zero-crossing detection of a lightweight dual-arm system connected to an aerial platform through a flexible beam is proposed. A similar approach has been employed in [5] for a 2-DoFs arm attached at the tip of a rigid one-meter-long link in a passive pendulum configuration.

To date, there is no published work about model-based control methods purposely designed for aerial cable-suspended robots that exploit the actuated load dynamics to dampen out the oscillatory behaviour of the system.

III. Control

Despite the many advantages of long-reach aerial manipulators discussed in Section I, with the employment of

flexible links unavoidable oscillations are induced in the system during and after the motion of the drone. The aim of the control problem is to use the cable-suspended anthropomorphic manipulator to suppress such oscillations by reducing the settling time and their amplitude. In solving this type of problem, the most challenging aspect from the control point of view is to deal with an underactuated system, i.e., a system that has fewer actuated DoFs than its total number. As a matter of fact, the model's joints associated to cables, located at the interfaces with the aerial platform and with the articulated system, do not have any actuation (passive joints) and cannot be directly controlled, but they still influence the dynamic behaviour of the whole system. In this section the control of the two robots (drone and articulated system) will be separated and we will only focus on the arms controller.

Underactuated systems are not feedback equivalent to a linear and decoupled system, i.e., cannot be fully feedback-linearised. Although we cannot always simplify the full dynamics of the system, it is still possible to linearise a portion of the system dynamics. The technique is called *partial feedback linearization* and it was first presented in [39]. The term *collocated* partial feedback linearization is used to describe a controller which linearises the dynamics of the actuated joints. However, under a condition regarding the degree of coupling between the active and passive joints, it is possible to achieve a *non-collocated* partial feedback linearization, i.e., a controller which linearises the dynamics of the unactuated joints [40].

The starting point of the control is the definition of the classical n-DoFs robot dynamic model formulation

$$B(q)\ddot{q} + n(q, \dot{q}) = G\tau, \tag{1}$$

with $(q, \dot{q})$, i.e. joints' position and velocity vector respectively, being the model state variables. In (1), $B \in \mathbb{R}^{n\times n}$ represents the mass matrix, $n \in \mathbb{R}^n$ is the nonlinear terms vector, i.e., gravity, centrifugal and Coriolis terms, while $G \in \mathbb{R}^{n\times m}$ is a suitable selection matrix to account for some joints being non-actuated. Without loss of generality, one can reorganise the joint coordinates in any underactuated system by highlighting the active and the passive parts, respectively referred to with the subscripts m and b, and rewrite (1) into the form

$$\begin{bmatrix} B_b & B_{bm} \\ B_{bm}^T & B_m \end{bmatrix} \begin{bmatrix} \ddot{q}_b \\ \ddot{q}_m \end{bmatrix} + \begin{bmatrix} n_b \\ n_m \end{bmatrix} = \begin{bmatrix} 0 \\ \tau_m \end{bmatrix}, \tag{2}$$

which is equivalent to

$$\begin{cases} B_b\ddot{q}_b + B_{bm}\ddot{q}_m + n_b = 0 \\ B_{bm}^T\ddot{q}_b + B_m\ddot{q}_m + n_m = \tau_m \end{cases}, \tag{3}$$

with $q_b \in \mathbb{R}^l$, $q_m \in \mathbb{R}^m$, $m = n - l$. The term B_b is an invertible $l \times l$ matrix as a consequence of the uniform positive definiteness of the robot inertia matrix B in (1), according to the necessary and sufficient condition of the generalised Schur complement [41]. It is then possible to isolate the term $\ddot{q}_b$ in the first equation of (3), and substitute it in the second one, thus obtaining

$$\underbrace{(B_m - B_{bm}^T B_b^{-1} B_{bm})}_{\tilde{B}}\ddot{q}_m + \underbrace{(n_b - B_{bm}^T B_b^{-1} n_m)}_{\tilde{n}} = \tau_m. \tag{4}$$

Since the cables are considered as a passive joints, i.e., unactuated joints, a non-collocated partial feedback linearization is considered. The term *non-collocated* means that the control acts on the passive joints instead of the active ones, meaning that the nonlinear dynamics of such joints are compensated, whereas those belonging to the active joints do not appear in the stabilisation control objective. Since it is possible to prove that $\tilde{B}$ in (4) is always invertible [39], an input/output feedback controller can be defined by choosing

$$\tau_m = \tilde{B}y_m + \tilde{n}. \tag{5}$$

Substituting (5) into (4), the dynamic model of the system becomes

$$\begin{cases} \ddot{q}_m = y_m \\ B_b\ddot{q}_b + n_b = -B_{bm}y_m \end{cases}. \tag{6}$$

If the matrix B_{bm} is full-rank, the underactuated system is said to be *strong inertially coupled*. If this property holds, the Moore-Penrose right pseudoinverse matrix of B_{bm} is well-defined and then, from the second equation in (6), y_m can be derived as

$$y_m = -B_{bm}^{\dagger}(B_b y_b + n_b), \tag{7}$$

where y_b is an additional control input yet to be determined. With this choice for the control input y_m, the system (6) becomes

$$\begin{cases} \ddot{q}_m = -B_{bm}^{\dagger}(B_b y_b + n_b) \\ \ddot{q}_b = y_b \end{cases}. \tag{8}$$

As the (8) reveals, the linearization of the unactuated part of the system has been achieved. The first equation of (8) represents instead the evolution of the internal zero dynamics. This means that controlling the behaviour of the linear part of the system is straightforward, for instance it is possible to use PD controller with acceleration feed-forward

$$y_b = \ddot{q}_b^d + K_d(\dot{q}_b^d - \dot{q}_b) + K_p(q_b^d - q_b). \tag{9}$$

leading to the closed-loop behavior described by the equation

$$\ddot{\tilde{q}}_b^d + K_d\dot{\tilde{q}}_b + K_p\tilde{q}_b = 0, \tag{10}$$

which is asymptotically stable, so the error tends to zero with a convergence speed depending on the choice of the matrices K_p and K_d. Hence, this framework allows to control the motion of the passive variables, even if there is no way to actuate them. For the resolution of the oscillation suppression task, it is sufficient to impose a constant zero reference for position, velocity and acceleration of the passive variables. The aim is to keep the cables vertical and the lower platform horizontal during the transportation phase (see Fig. 2).

Since the zero dynamics is uncontrolled, a term in the null-space of the coupling inertia matrix has been added so that the manipulators remain as close as possible to the initial rest

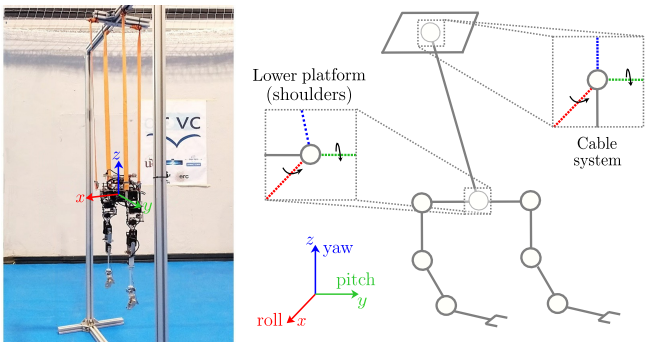

Fig. 2. Left: robot suspended through 4-cables configuration on a testbed. Right: graphical representation of the aerial robot in a generic configuration. Detail on cable suspension system and lower platform (i.e. shoulders) which always remain horizontal to the ground thanks to the cables parallel pattern.

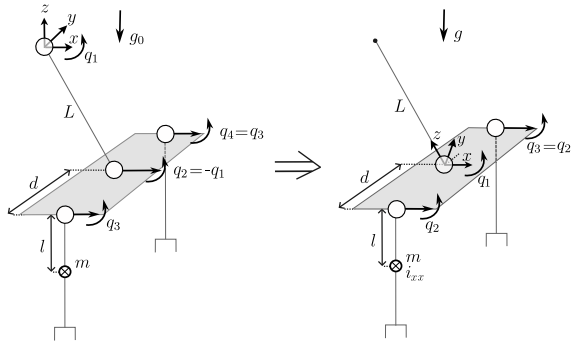

Fig. 3. Left: starting reduced model, with fixed base frame with origin coincident with the cables' upper suspension point. Right: modified proposed reduced model, with base frame's origin integral to the cables and origin coincident with the cables' lower connection point.

configuration q_{m_0}. This reduces the occurrence of unstable internal dynamics. Equation (7) then becomes

$$\begin{aligned} y_m = &- B_{bm}^{\dagger}(B_b y_b + n_b) + (I - B_{bm}^{\dagger} B_{bm}) \\ &[G_d(-\dot{q}_m) + G_p(q_{m_0} - q_m)]. \end{aligned} \tag{11}$$

Hence, the actual control is the combination of (5) and (11).

IV. Reduced Models

As explained in Section III, a central node for the control to work is the strong inertial coupling property, which is strictly related to the rank of the coupling matrix B_{bm}. By the time one goes to use a complete model of the system, whose definition has been presented in [42], it has been numerically verified that this property is not always respected. To demonstrate this analytically in an easily understandable manner, let us examine without lost of generality a foundation model (see Fig. 3, left), conceptually akin to the complete one, featuring some simplifying assumption. In particular: (i) the arms are represented as a single rigid link rotating around the shoulder structure; (ii) only rotational movements orthogonal to the $y - z$ plane are addressed, i.e., joints $q_1 \dots q_4$; (iii) the upper and lower passive joint state variables q_1 and q_2 have identical magnitudes but opposite signs due to the horizontal platform behaviour imposed by cable constraints (as discussed in [42]); (iv) the arms are supposed to move identically, i.e. the state variables q_3 and q_4 are combined. Under these assumptions, the model reduces to a 4-DoFs system whose dynamics is described by the equation

$$\begin{pmatrix} b_{11} & b_{12} & b_{13} & b_{14} \\ b_{21} & b_{22} & b_{23} & b_{24} \\ b_{31} & b_{32} & b_{33} & 0 \\ b_{41} & b_{42} & 0 & b_{43} \end{pmatrix} \begin{pmatrix} \ddot{q}_1 \\ \ddot{q}_2 \\ \ddot{q}_3 \\ \ddot{q}_4 \end{pmatrix} + \begin{pmatrix} n_1 \\ n_2 \\ n_3 \\ n_4 \end{pmatrix} = \begin{pmatrix} 0 \\ 0 \\ \tau_3 \\ \tau_4 \end{pmatrix} \tag{12}$$

where, on the basis of the assumptions made $\{q_2, \dot{q}_2, \ddot{q}_2\} = \{\text{-}q_1, \text{-}\dot{q}_1, \text{-}\ddot{q}_1\}$ and $\{q_4, \dot{q}_4, \ddot{q}_4, \tau_4\} = \{q_3, \dot{q}_3, \ddot{q}_3, \tau_3\}$. In this case, the dynamic coupling matrix $B_{bm} = [b_{13}, b_{14};\ b_{23}, b_{24}]$, and the terms are specified as follows

$$\begin{cases} b_{13} = i_{xx} + ml^2 + mLl\cos(q_3 - q_1) + mld\sin(q_3) \\ b_{14} = i_{xx} + ml^2 + mLl\cos(q_3 - q_1) - mld\sin(q_3) \\ b_{23} = i_{xx} + ml^2 + mld\sin(q_3) \\ b_{24} = i_{xx} + ml^2 - mld\sin(q_3) \end{cases}. \tag{13}$$

It is easy to verify that the determinant of B_{bm} is equal to

$$\det(B_{bm}) = -2m^2Ll^2d\cos(q_3 - q_1)\sin q_3, \tag{14}$$

thus, for the rank to be full, the following condition must be satisfied

$$\begin{aligned} &\cos(q_3 - q_1) \neq 0 \quad \wedge \quad \sin q_3 \neq 0 \quad \Rightarrow \\ \Rightarrow \quad &q_3 \neq \pi/2 + q_1 + k\pi \quad \wedge \quad q_3 \neq k\pi. \end{aligned} \tag{15}$$

While the former is not a condition of interest, since it involves the arms being extended sideways to form a square angle, the latter is a working condition since it corresponds to the case where the arms are aligned downwards.

It is therefore necessary to search for a different simplified model that allows the condition of strong inertial coupling to be fulfilled everywhere. On the right of Fig. 3, a model is presented in which the world frame is integral with the cables, with origin coinciding with the origin of the spherical joint attached to the shoulders. Since the shoulder structure is always parallel to the ground, it is easy to verify how geometrically the angle formed by the cables with respect to a vertical axis corresponds identically to the angle formed by the shoulders with respect to the cables, with opposite sign. The control objective can then be converted into an objective of controlling the position of the shoulders in relation to the cables, rather than the cables themselves. The reduced model becomes a 3-DoFs system, where the first joint is passive and the other two (arms joints) are active. Exploiting assumptions (i)-(iv), we obtain the following dynamic model

$$\begin{pmatrix} b_{11} & b_{12} & b_{13} \\ b_{21} & b_{22} & 0 \\ b_{31} & 0 & b_{33} \end{pmatrix} \begin{pmatrix} \ddot{q}_1 \\ \ddot{q}_2 \\ \ddot{q}_3 \end{pmatrix} + \begin{pmatrix} n_1 \\ n_2 \\ n_3 \end{pmatrix} = \begin{pmatrix} 0 \\ \tau_2 \\ \tau_3 \end{pmatrix} \tag{16}$$

where $\{q_3, \dot{q}_3, \ddot{q}_3, \tau_3\} = \{q_2, \dot{q}_2, \ddot{q}_2, \tau_2\}$. The values of interest of the dynamic coupling matrix $B_{bm} = [b_{12}, b_{13}]$ this time can be written as

$$\begin{cases} b_{12} = i_{xx} + ml^2 + mld\sin(q_2) \\ b_{13} = i_{xx} + ml^2 - mld\sin(q_2) \end{cases}. \tag{17}$$

The rank of the B_{bm} matrix is verified from the analysis of

$$\begin{aligned} \det(B_{bm}B_{bm}^T) = &\ 2i_{xx}^2 + 2m^2l^4 \\ &+ 4i_{xx}ml^2 + 2(mld\sin q_2)^2, \end{aligned} \tag{18}$$

which now can never take on a null value since all parameters in the equation are strictly greater than zero, i.e. all terms are strictly positive. It is important to note that, since the base frame is integral with the cables, the gravity acceleration vector g does not result always parallel to the z-axis, as is possible to see in Fig. 3. To obtain the correct model representation expressed in the base frame, the vector must therefore be appropriately rotated as follows

$$g = \begin{pmatrix} g_0 \sin(q_1) \\ 0 \\ -g_0 \cos(q_1) \end{pmatrix}. \tag{19}$$

Similar considerations apply to derive the overall model integrating oscillations around the two axes x and y and with a complete kinematic model of the arms.

V. Experimental setup and control results

As mentioned in Section I, the control was first tested in a simulation environment and later transferred to the real system. This section describes the experimental setup used to test the control (Section V-A), the simulation results obtained (Section V-B), and finally the results of the experiments conducted on the real system (Section V-C).

A. Experimental setup

The platform used to validate experimentally the methods described before consists of a lightweight and compliant anthropomorphic dual arm system (LiCAS A1[1]) suspended from a medium-size quadrotor by four cables in *puppet* configuration (1 m length, 250 mm separation), as shown in Fig. 1(a). The arms, built with smart servo actuators and a frame structure manufactured in carbon fiber and aluminium, are human-size (500 mm reach, 360 mm arms separation) and human-like, with three joints at the shoulder and one at the elbow in the usual anthropomorphic kinematics [43]. The total weight of the manipulator is 3 kg, with 0.5 kg payload capacity. The multi-rotor is based on the Tarot X4 quadrotor frame, with DJI E2000 motors and 21×7 inch propellers, implementing the controller on a Pixhawk 2 [44]. This quadrotor, weighting 5 kg, provides a maximum take-off weight around 9 kg, with a maximum flight time of 45 min with no load, and 5 - 10 min with the integrated arms.

Unlike the single or double cable configuration (slung-swing load), the four cable arrangement avoids that the shoulder structure is tilted in roll or pitch due to the reaction moment exerted by the rotation of the left and/or right arms, as long as the center of mass of the arms is within the polygon defined by the four anchor points of the cables. Also, unlike the flexible long reach links used in our previous works [5], [7] that tend to induce lateral moments with non-minimum phase zeros on the multi-rotor controller, cables only transmit forces, that tend to disturb less the platform and do not compromise stability due to lateral forces [5]. The length of the cables and their separation are determined empirically taking into account the safety distance and the oscillation frequency of the slung manipulator, as well as integration constraints imposed by landing gear of the multirotor.

[1]https://licas-robotic-arms.com/

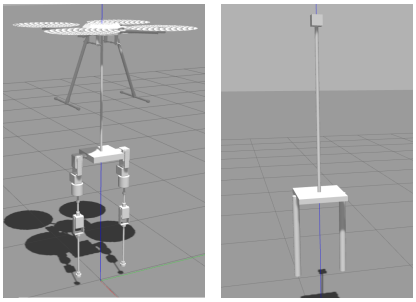

(a) (b)

Fig. 4. Gazebo simulation environment containing the (a) full model of the cable-suspended UAM system under study and (b) its reduced version.

Experiments were conducted at the GRVC Aerial Robotics Laboratory indoor testbed, which is equipped with 28 OptiTrack cameras. The multi-rotor and the shoulder structure of the LiCAS incorporate passive infrared markers to measure the position of both bodies with sub-centimetre accuracy, hence allowing the computation of cables' inclination from the vertical rest configuration. The controller of the arms is implemented on a Raspberry Pi 3B computer board, receiving through UDP sockets the references computed by the ground control station laptop that receives the data from OptiTrack.

B. Simulation results

Before applying the control strategy to the real system, a simulation environment was developed using Gazebo (ROS), in order to prevent damage to the real structure and test the control in a secure way. In [42] a simulation environment for the complete model has been developed, as showed in Fig. 4(a). In order to be consistent with the reduced models presented in Section IV, the simulated system was suitably modified as shown in Fig. 4(b). In the simulation, the four cables have been represented as a single unactuated rigid link. The horizontality behaviour of the shoulders, instead, has been reproduced through a virtual revolute joint controlled such that it keeps the shoulder structure always parallel to the ground. It should finally be noticed that the simulation does not take into account any of the external forces happening on the aerial platform when the system is moving, i.e., wind disturbances or contacts.

As a first approach, the simulation has been developed supposing the system to hang from a fixed structure, i.e. the upper suspension platform was modelled as a fixed joint. The oscillations to suppress are forced exploiting the action of gravity through an initial angular displacement of 0.15 rad along x and y axes in turn. Figure 5a shows the comparison between the oscillations, measured as the angle of the cables' link with respect to their rest condition, with and without control, in the case of a swing generated through a non-zero initial displacement around x-axis. The shoulder roll joints (abduction/adduction rotation) have been used for the control. Mechanical constraints on the LiCAS, i.e. joint

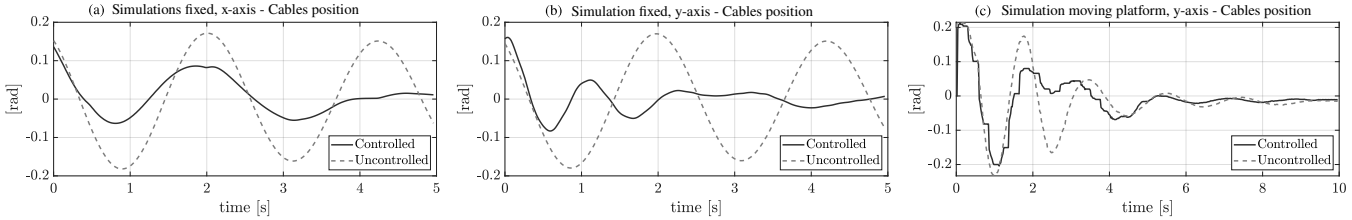

Fig. 5. Cables angular displacement with respect to a vertical rest condition for comparisons between uncontrolled (dotted line) and controlled (solid line) simulations for oscillations (a) around x-axis with fixed suspension platform, (b) around y-axis with fixed suspension platform, (c) around y-axis with linearly moving suspension platform.

limits, are imposed to prevent the collision of the arms with the shoulder structure or between them. In particular, the rotation angle into the shoulder structure of the roll joints is limited to 20 deg.

Despite the imposed limit, Fig. 5(a) highlights a faster oscillation suppression thanks to the employment of the control. The error becomes zero at steady state and the oscillation amplitude is approximately reduced by 47% in 2 seconds, while the settling time is about 4 seconds. The energy consumption needed to apply this control input u, i.e., active joints control torque, evaluated as

$$E = \int u^2(t)dt, \tag{20}$$

amounts to 11.5 J which is quite favourable, particularly when compared to the usage of LiPo batteries on the real system, which have a capacity of 1.26×10^5 J.

Figure 5(b) instead shows the case of a simulation in which the initial displacement is non-zero only along the y-axis. This time, the idea is to use the shoulder pitch joints for the control. This configuration allows the removal of the previous constraint since there is no physical obstruction when the joint rotates around the joints' axes. It is easy to appreciate the reduction of the amplitude of the oscillations with respect to the previous case. At 2.5 seconds, now, the amplitude is reduced by 87% and the settling time is around 2.7 seconds. Also, the control input appears to be lower than in the previous case, due to the lack of constraints and accordingly the energy consumption, which is equal to 1.89 J.

At a later time the simulations have been enriched by inserting the moving suspension platform, modelled as a prismatic joint, to mimic the presence of the drone. The idea is to independently move the aerial platform to a desired point, and subsequently use the arms to suppress the oscillation. In this configuration, the drone has been controlled in simulation with a simple PID to follow a desired 1 meter linear trajectory. Figure 5(c) shows the obtained results for a movement of the drone along the x-axis. We still have a great reduction of the amplitude of the oscillation, which is about 76% and the settling time is around 5 seconds. Also, the control energy reaches 238.7 J.

C. Experimental results on the physical system

As with the simulations, in order to validate the results shown in Section V-B, the experiments on the physical system were carried out in two different phases: in the first, the dual arm was suspended from a fixed testbed, whereas in the second, the arms were tested on flight. Figure 6(a)-(c) shows the results of an experiment in which oscillations around x-axis are generated, hence shoulder roll joints are employed for the control. As it can be noticed in Fig. 6(a), the oscillations are suppressed in approximately 5 seconds, the reduction of the amplitude is approximately 54% and the evaluated control energy is equal to 4.26 J. Figures 6(b) and 6(c) show the torque control inputs (evaluated from motors' current measures) and joints' measured velocities. As described in Section V-B, the shoulder roll structure cannot be moved towards the lower platform with an angle bigger than 20 degrees. Secondly an experiment was made by making the system oscillate around the y-axis and by controlling the shoulder pitch structure. In this configuration, the position limits applied before are no longer needed, because the joint can freely rotate. As can be seen in Fig. 6(f) experimental trials suggested in this case to impose velocity limits on the joints to avoid abrupt movements. The results in Fig. 6(d), show the amplitude of the oscillations to be reduced by 87% in 4 seconds, with an evaluated control energy of 370.8 J. Even though the energy required for this controller is higher than in the previous case, it is still very low with respect to the used batteries' capacity and it might still be worth trading, since it allows the system to reach the desired position in a very short time.

Subsequently, the fixed structure has been replaced by the aerial platform. Without any control applied to the arms, when the drone moves, we expect it to induce oscillations on the cables. However, since the damping of the system is really high, such oscillations are partially absorbed by the aerial platform more quickly with respect to the fixed base case. Figure 6(g) shows the comparison between an uncontrolled experiment and the data obtained by activating the arms control. In this case, all of the previous precautions have been considered, e.g. the control around the y-axis to avoid position limits and the application of velocity limits, instead, on the arms' joints. It is worth noticing that, for the control, the model described in Section IV with an additional prismatic upper joint has been adopted. We can state that the control of the arms helps the suppression oscillation by both reducing the settling time to 2.5 seconds and the amplitude by 89%. In this case, the evaluated control energy is of 476.97 J. Finally, Fig. 7 reports a sequence of images from all of the tests performed on the real system,

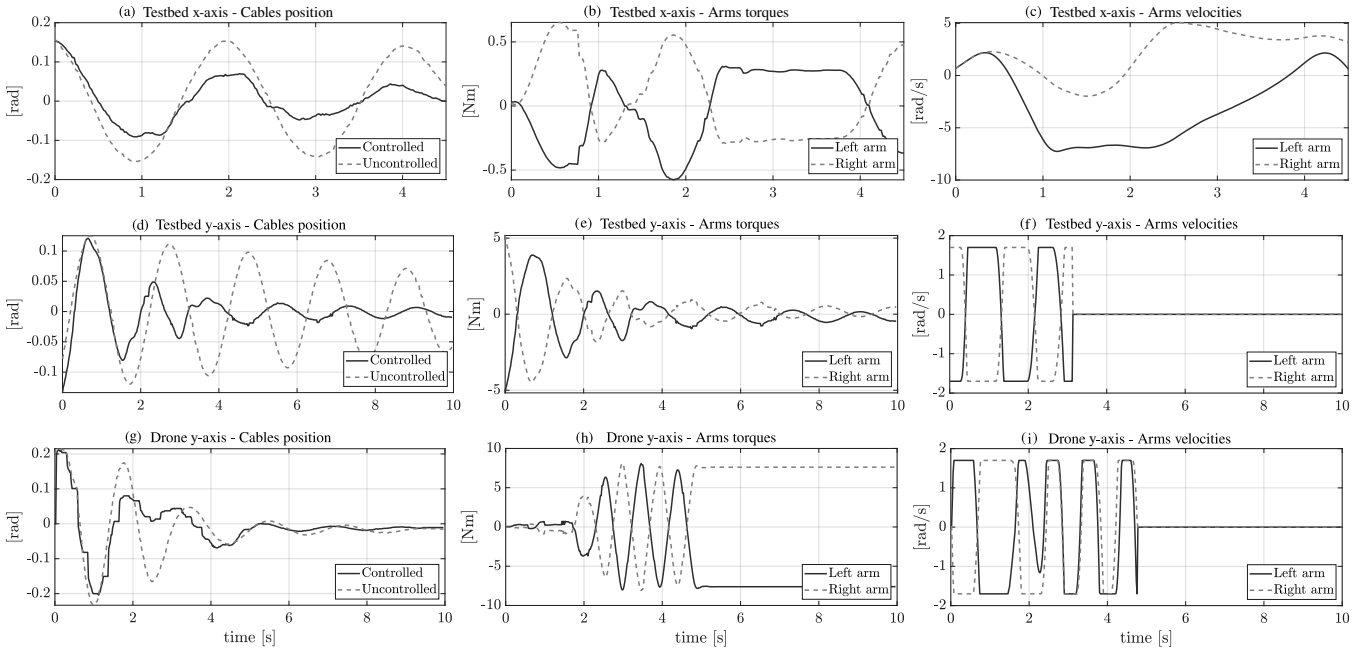

Fig. 6. Experiments on physical system with dual-arm manipulator. Left column shows the comparison between cable position with and without control, central column shows torque inputs for arms joints, and finally right column shows joints' measured velocities. (a)-(c) Suspension from a testbed for an oscillation around x-axis with shoulder roll joint actuation. (d)-(f) Suspension from a testbed for an oscillation around y-axis with shoulder pitch joint actuation. (g)-(i) Suspension from a drone linearly moving along x-axis (oscillation around y) with shoulder pitch joint actuation.

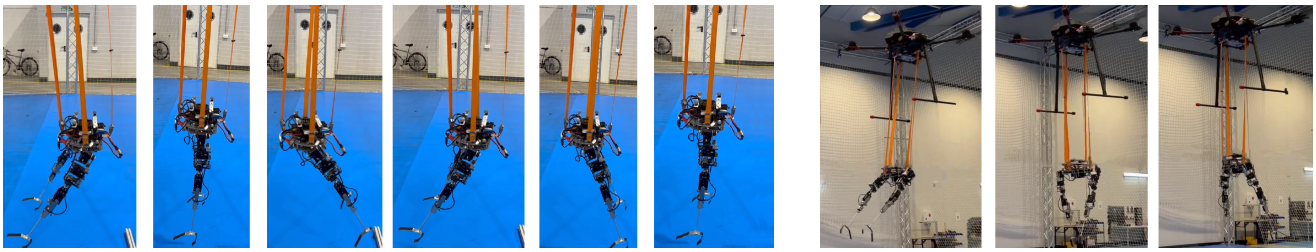

(a) (b)

Fig. 7. Sequence of images from the experiments on the physical system: (a) control test with system hanging from a testbed, (b) control test with full system and drone motion.

in particular Fig. 7(a) shows the experiments on the testbed while Fig. 7(b) the ones with the one involving the drone transportation.

VI. Conclusions and Discussion

In this study, an innovative control strategy for aerial cable-suspended dual-arm systems was developed and tested with the aim of mitigating oscillations due to the presence of the cables. Employing a non-collocated partial feedback linearization control technique we were able to reduce the oscillation amplitudes induced by drone motion by up to 89%, with a settling time of 2.5 seconds. The proposed technique relies on reduced dynamic models of the system, which were devised to respect the strong inertial coupling condition and, simultaneously, allow a straightforward simulation of the system. From the analysis of the experimental results, we found the energy consumption to achieve these results very limited, demonstrating the feasibility of the control within the system's battery capacity.

Potential improvements include a more comprehensive modelling including all the system's joints to control oscillations in all directions. In future works, we aim to test the controller in real-world scenarios, without a visual system, and ensure robustness in unpredictable conditions. Finally, the coordinated control between the two robots, drone and articulated system, is also considered, emphasising ongoing efforts to enhance system robustness and applicability for diverse tasks.

References

[1] A. Ollero, M. Tognon, A. Suarez, D. Lee, and A. Franchi, "Past, present, and future of aerial robotic manipulators," *IEEE Transactions on Robotics*, vol. 38, no. 1, pp. 626–645, 2022.

[2] F. Ruggiero, V. Lippiello, and A. Ollero, "Aerial manipulation: A literature review," *IEEE Robotics and Automation Letters*, vol. 3, no. 3, pp. 1957–1964, 2018.

[3] A. Ollero, G. Heredia, A. Franchi, G. Antonelli, K. Kondak, A. Sanfeliu, A. Viguria, J. R. Martinez-de Dios, F. Pierri, J. Cortés, *et al.*, "The aeroarms project: Aerial robots with advanced manipulation capabilities for inspection and maintenance," *IEEE Robotics & Automation Magazine*, vol. 25, no. 4, pp. 12–23, 2018.

[4] M. Di Castro, M. Ferre, and A. Masi, "Cerntauro: A modular architecture for robotic inspection and telemanipulation in harsh and semi-structured environments," *IEEE Access*, vol. 6, pp. 37506–37522, 2018.

[5] A. Suárez, P. Sanchez-Cuevas, M. Fernandez, M. Perez, G. Heredia, and A. Ollero, "Lightweight and compliant long reach aerial manipulator for inspection operations," in *2018 IEEE/RSJ International Conference on Intelligent Robots and Systems*, pp. 6746–6752, IEEE, 2018.

[6] Y. S. Sarkisov, M. J. Kim, D. Bicego, D. Tsetserukou, C. Ott, A. Franchi, and K. Kondak, "Development of sam: cable-suspended aerial manipulator," in *2019 IEEE International Conference on Robotics and Automation*, pp. 5323–5329, 2019.

[7] A. Suarez, F. Real, V. M. Vega, G. Heredia, A. Rodriguez-Castaño, and A. Ollero, "Compliant bimanual aerial manipulation: Standard and long reach configurations," *IEEE Access*, vol. 8, pp. 88844–88865, 2020.

[8] A. Suarez, R. Salmoral, P. J. Zarco-Periñan, and A. Ollero, "Experimental evaluation of aerial manipulation robot in contact with 15 kv power line: Shielded and long reach configurations," *IEEE Access*, vol. 9, pp. 94573–94585, 2021.

[9] I. Armengol, A. Suarez, G. Heredia, and A. Ollero, "Design, integration and testing of compliant gripper for the installation of helical bird diverters on power lines," in *2021 Aerial Robotic Systems Physically Interacting with the Environment*, pp. 1–8, 2021.

[10] J. Cacace, S. M. Orozco-Soto, A. Suarez, A. Caballero, M. Orsag, S. Bogdan, G. Vasiljevic, E. Ebeid, J. A. A. Rodriguez, and A. Ollero, "Safe local aerial manipulation for the installation of devices on power lines: Aerial-core first year results and designs," *Applied Sciences*, vol. 11, no. 13, p. 6220, 2021.

[11] L. R. Arms, "https://licas-robotic-arms.com/ (accessed: 05.02.2024)."

[12] C. D. Bellicoso, L. R. Buonocore, V. Lippiello, and B. Siciliano, "Design, modeling and control of a 5-dof light-weight robot arm for aerial manipulation," in *2015 23rd Mediterranean Conference on Control and Automation (MED)*, pp. 853–858, IEEE, 2015.

[13] T. Bartelds, A. Capra, S. Hamaza, S. Stramigioli, and M. Fumagalli, "Compliant aerial manipulators: Toward a new generation of aerial robotic workers," *IEEE Robotics and Automation Letters*, vol. 1, no. 1, pp. 477–483, 2016.

[14] Z. Ouyang, R. Mei, Z. Liu, M. Wei, Z. Zhou, and H. Cheng, "Control of an aerial manipulator using a quadrotor with a replaceable robotic arm," in *2021 IEEE International Conference on Robotics and Automation*, pp. 153–159, 2021.

[15] R. Miyazaki, R. Jiang, H. Paul, Y. Huang, and K. Shimonomura, "Long-reach aerial manipulation employing wire-suspended hand with swing-suppression device," *IEEE Robotics and Automation Letters*, vol. 4, no. 3, pp. 3045–3052, 2019.

[16] J. Lee, R. Balachandran, Y. S. Sarkisov, M. De Stefano, A. Coelho, K. Shinde, M. J. Kim, R. Triebel, and K. Kondak, "Visual-inertial telepresence for aerial manipulation," in *2020 IEEE International Conference on Robotics and Automation*, pp. 1222–1229, 2020.

[17] G. Loianno, V. Spurny, J. Thomas, T. Baca, D. Thakur, D. Hert, R. Penicka, T. Krajnik, A. Zhou, A. Cho, *et al.*, "Localization, grasping, and transportation of magnetic objects by a team of mavs in challenging desert-like environments," *IEEE Robotics and Automation Letters*, vol. 3, no. 3, pp. 1576–1583, 2018.

[18] M. Mohammadi, D. Bicego, A. Franchi, D. Barcelli, and D. Prattichizzo, "Aerial tele-manipulation with passive tool via parallel position/force control," *Applied Sciences*, vol. 11, no. 19, 2021.

[19] D. Qian, *Anti-sway control for cranes: design and implementation using MATLAB*. De Gruyter, 2017.

[20] K.-S. Hong and U. H. Shah, *Dynamics and control of industrial cranes*. Springer, 2019.

[21] H. Li, Y.-B. Hui, Q. Wang, H.-X. Wang, and L.-J. Wang, "Design of anti-swing pid controller for bridge crane based on pso and sa algorithm," *Electronics*, vol. 11, no. 19, p. 3143, 2022.

[22] C.-Y. Chang, "Adaptive fuzzy controller of the overhead cranes with nonlinear disturbance," *IEEE transactions on industrial informatics*, vol. 3, no. 2, pp. 164–172, 2007.

[23] Q. H. Ngo and K.-S. Hong, "Sliding-mode antisway control of an offshore container crane," *IEEE/ASME transactions on mechatronics*, vol. 17, no. 2, pp. 201–209, 2010.

[24] D. Jolevski and O. Bego, "Model predictive control of gantry/bridge crane with anti-sway algorithm," *Journal of mechanical science and technology*, vol. 29, pp. 827–834, 2015.

[25] N. Sun, Y. Wu, Y. Fang, and H. Chen, "Nonlinear antiswing control for crane systems with double-pendulum swing effects and uncertain parameters: Design and experiments," *IEEE Transactions on Automation Science and Engineering*, vol. 15, no. 3, pp. 1413–1422, 2017.

[26] M. J. Maghsoudi, Z. Mohamed, S. Sudin, S. Buyamin, H. Jaafar, and S. Ahmad, "An improved input shaping design for an efficient sway control of a nonlinear 3d overhead crane with friction," *Mechanical Systems and Signal Processing*, vol. 92, pp. 364–378, 2017.

[27] S. Garrido, M. Abderrahim, A. Gimenez, R. Diez, and C. Balaguer, "Anti-swinging input shaping control of an automatic construction crane," *IEEE Transactions on Automation Science and Engineering*, vol. 5, no. 3, pp. 549–557, 2008.

[28] Q. Chen, W. Cheng, L. Gao, and J. Fottner, "A pure neural network controller for double-pendulum crane anti-sway control: Based on lyapunov stability theory," *Asian Journal of Control*, vol. 23, no. 1, pp. 387–398, 2021.

[29] X. Lan, L. Gong, L. Zheng, S. Liu, and W. Xu, "Anti-swing strategy of a quadrotor with suspended payload based on model predictive control," in *2023 9th International Conference on Control Science and Systems Engineering (ICCSSE)*, pp. 20–25, IEEE, 2023.

[30] H. M. Omar and S. M. Mukras, "Integrating anti-swing controller with px4 autopilot for quadrotor with suspended load," *Journal of Mechanical Science and Technology*, vol. 36, no. 3, pp. 1511–1519, 2022.

[31] F. Ding, C. Sun, and S. He, "Anti-swing control for quadrotor-slung load transportation system with underactuated state constraints," *Sensors*, vol. 23, no. 21, p. 8995, 2023.

[32] X. Liang, K. Cai, and J. Han, "Anti-swing trajectory planning for quadrotor transportation systems with double-pendulum swing effects," in *Advances in Applied Nonlinear Dynamics, Vibration and Control-2021: The proceedings of 2021 International Conference on Applied Nonlinear Dynamics, Vibration and Control*, pp. 875–887, Springer, 2022.

[33] P. Homolka, M. Hromčík, and T. Vyhlídal, "Input shaping solutions for drones with suspended load: First results," in *2017 21st International Conference on Process Control*, pp. 30–35, IEEE, 2017.

[34] H. Kawai, Y. B. Kim, and Y. W. Choi, "Anti-sway system with image sensor for container cranes," *Journal of mechanical science and technology*, vol. 23, pp. 2757–2765, 2009.

[35] C. W. Kim, K.-S. Hong, and G. Lodewijks, "Anti-sway control of container cranes: an active mass-damper approach," in *SICE 2004 annual conference*, vol. 1, pp. 939–944, IEEE, 2004.

[36] G. D'Ago, M. Lefebvre, L. R. Buonocore, F. Ruggiero, M. Di Castro, and V. Lippiello, "Modelling and control of a variable-length flexible beam on inspection ground robot," in *2022 International Conference on Robotics and Automation*, pp. 8224–8230, IEEE, 2022.

[37] R. Lampariello, J. Heindl, R. Koeppe, and G. Hirzinger, "Reactionless control for two manipulators mounted on a cable-suspended platform," in *2006 International Conference on Intelligent Robots and Systems*, pp. 91–97, 2006.

[38] A. Suárez, A. M. Giordano, K. Kondak, G. Heredia, and A. Ollero, "Flexible link long reach manipulator with lightweight dual arm: Soft-collision detection, reaction, and obstacle localization," in *2018 IEEE International Conference on Soft Robotics*, pp. 406–411, IEEE, 2018.

[39] M. W. Spong, "Partial feedback linearization of underactuated mechanical systems," in *IEEE/RSJ International Conference on Intelligent Robots and Systems*, vol. 1, pp. 314–321, IEEE, 1994.

[40] R. Tedrake, "Underactuated robotics: Learning, planning, and control for efficient and agile machines course notes for mit 6.832," *Working draft edition*, vol. 3, no. 4, p. 2, 2009.

[41] F. Zhang, *The Schur complement and its applications*, vol. 4. Springer Science & Business Media, 2006.

[42] G. D'Ago, M. Selvaggio, A. Suarez, F. J. Gañán, L. R. Buonocore, M. Di Castro, V. Lippiello, A. Ollero, and F. Ruggiero, "Modelling and identification methods for simulation of cable-suspended dual-arm robotic systems," *Robotics and Autonomous Systems*, p. 104643, 2024.

[43] A. Suarez, G. Heredia, and A. Ollero, "Design of an anthropomorphic, compliant, and lightweight dual Arm for aerial manipulation," *IEEE Access*, vol. 6, pp. 29173–29189, 2018.

[44] A. Suarez, H. Romero, R. Salmoral, J. A. Acosta, J. Zambrano, and A. Ollero, "Experimental evaluation of aerial manipulation robot for the installation of clip type bird diverters: Outdoor flight tests," in *2021 Aerial Robotic Systems Physically Interacting with the Environment*, pp. 1–7, IEEE, 2021.